



Published in final edited form as:

*Pac Symp Biocomput.* 2013 ; : 188–199.

## CHARACTERIZATION OF THE METABOCHIP IN DIVERSE POPULATIONS FROM THE INTERNATIONAL HAPMAP PROJECT IN THE EPIDEMIOLOGIC ARCHITECTURE FOR GENES LINKED TO ENVIRONMENT (EAGLE) PROJECT

### DANA C. CRAWFORD,

Department of Molecular Physiology and Biophysics, Center for Human Genetics Research, Vanderbilt University, 2215 Garland Avenue, 519 Light Hall Nashville, TN 37232, USA  
crawford@chgr.mc.vanderbilt.edu

### ROBERT GOODLOE,

Center for Human Genetics Research, Vanderbilt University, 2215 Garland Avenue, 519 Light Hall Nashville, TN 37232, USA robert.j.goodloe@vanderbilt.edu

### KRISTIN BROWN-GENTRY,

Center for Human Genetics Research, Vanderbilt University, 1207 17<sup>th</sup> Avenue, Suite 300 Nashville, TN 37232, USA kristin.brown@chgr.mc.vanderbilt.edu

### SARAH WILSON,

Center for Human Genetics Research, Vanderbilt University, 1207 17<sup>th</sup> Avenue, Suite 300 Nashville, TN 37232, USA sarah.wilson@chgr.mc.vanderbilt.edu

### JAMIE ROBERSON,

Center for Human Genetics Research, Vanderbilt University, 2215 Garland Avenue, 519 Light Hall Nashville, TN 37232, USA jamie.l.roberson@vanderbilt.edu

### NILOUFAR B. GILLANI,

Center for Human Genetics Research, Vanderbilt University, 2215 Garland Avenue, 519 Light Hall Nashville, TN 37232, USA nila.gillani@vanderbilt.edu

### MARYLYN D. RITCHIE,

Department of Biochemistry and Molecular Biology, Center for System Genomics, Pennsylvania State University, 512 Wartik Lab University Park, PA 16802, USA marylyn.ritchie@psu.edu

### HOLLI H. DILKS, and

Department of Molecular Physiology and Biophysics, Center for Human Genetics Research, Vanderbilt University, 2215 Garland Avenue, 519 Light Hall Nashville, TN 37232, USA  
holli.dilks@chgr.mc.vanderbilt.edu

### WILLIAM S. BUSH

Department of Biomedical Informatics, Center for Human Genetics Research, Vanderbilt University, 2215 Garland Avenue, 519 Light Hall Nashville, TN 37232, USA  
william.s.bush@vanderbilt.edu

## Abstract

Genome-wide association studies (GWAS) have identified hundreds of genomic regions associated with common human disease and quantitative traits. A major research avenue for mature genotype-phenotype associations is the identification of the true risk or functional variant for downstream molecular studies or personalized medicine applications. As part of the Population Architecture using Genomics and Epidemiology (PAGE) study, we as Epidemiologic Architecture for Genes Linked to Environment (EAGLE) are fine-mapping GWAS-identified genomic regions

for common diseases and quantitative traits. We are currently genotyping the MetaboChip, a custom content BeadChip designed for fine-mapping metabolic diseases and traits, in ~15,000 DNA samples from patients of African, Hispanic, and Asian ancestry linked to deidentified electronic medical records from the Vanderbilt University biorepository (BioVU). As an initial study of quality control, we report here the genotyping data for 360 samples of European, African, Asian, and Mexican descent from the International HapMap Project. In addition to quality control metrics, we report the overall allele frequency distribution, overall population differentiation (as measured by  $F_{ST}$ ), and linkage disequilibrium patterns for a select GWAS-identified region associated with low-density lipoprotein cholesterol levels to illustrate the utility of the MetaboChip for fine-mapping studies in the diverse populations expected in EAGLE, the PAGE study, and other efforts underway designed to characterize the complex genetic architecture underlying common human disease and quantitative traits.

---

## 1. Introduction

In the last seven years, genome-wide association studies (GWAS) have been used extensively to identify common genetic variants associated with human diseases and quantitative traits. While there are many replicated and mature, known relationships between genomic regions and phenotypes, very few individual genetic variants have been identified as the risk variant for downstream molecular studies or personalized medicine applications. The lack of true functional variants revealed by GWAS stems from the fact that GWAS is based on linkage disequilibrium (LD), the non-random association of alleles at different variants along the chromosome. That is, GWAS fixed-content products mostly assay presumably neutral common genetic variants that are in LD or “tag” other genetic variants not directly assayed resulting in GWAS-identified regions that probably contain the true risk (unassayed) variant.

To identify the true risk variant, a major proposed activity in the “post-GWAS” era is *fine mapping*. In a fine-mapping experiment, the GWAS-identified region is densely interrogated via thousands of common and rare variants. Fine-mapping experiments can also take advantage of the known LD differences observed across populations. For example, populations of African-descent have lower levels of LD compared with populations of European-descent and therefore may be useful in identifying the risk variant masked by higher levels of LD in other populations. Fine mapping across populations is also useful for identifying population-specific variants associated with phenotypes.

In recognition for the need to fine-map mature GWAS-identified regions originally identified in European-descent populations, the National Human Genome Research Institute established the Population Architecture using Genomics and Epidemiology (PAGE) study to genotype African American and Asian populations linked to phenotypes using the Illumina MetaboChip, a custom iSelect BeadChip designed to fine-map GWAS-identified regions for metabolic diseases and traits. We as Epidemiologic Architecture for Genes Linked to Environment (EAGLE) are genotyping ~15,000 DNA samples linked to de-identified electronic medical records in the Vanderbilt University biorepository (BioVU) for fine mapping within the PAGE study. As the first step in quality control, EAGLE has genotyped 360 HapMap samples from European, African, Asians, and Mexican-descent populations. This short report describes the quality control, variant properties, and the potential for fine mapping of GWAS-identified regions in the anticipated populations within EAGLE and the PAGE study.

## 2. Methods

### 2.1. Study populations

DNA samples were obtained by the PAGE Coordinating Center from the Coriell Cell Repositories<sup>1</sup>. A total of 360 samples overlapping the International HapMap Project collection were obtained, including 30 trios of Northern and Western European ancestry from Utah from the Centre d'Etude du Polymorphisme Humain (CEPH) collection (CEU; catalog ID HAPMAPPT01), 90 unrelated individuals representing 45 individuals each from Tokyo, Japan and Beijing, China (ASN; catalog ID HAPMAPPT02), 30 trios from the Yoruba in Ibadan, Nigeria (YRI; catalog ID HAPMAPPT03), and 30 trios from communities of Mexican origin in Los Angeles, California (MEX; catalog ID HAPMAPV13). Samples were chosen to reflect the overall genetic ancestry of epidemiologic and clinical-based samples available in the PAGE study<sup>1</sup>.

### 2.2. Genotyping

Aliquots of HapMap DNA samples were distributed by the PAGE Coordinating Center to individual PAGE study sites. The Vanderbilt DNA Resources Core genotyped the Illumina MetaboChip on the HapMap samples distributed by the PAGE Coordinating Center on the Illumina iScan (San Diego, California). The MetaboChip is a custom BeadChip targeting 196,725 genetic variants. Common and less common genetic variants were chosen from among the first iteration of the 1000 Genomes Project and represent index GWAS-identified variants regardless of disease or phenotype as of 2009; regions targeted for fine-mapping for specific GWAS-identified regions associated with coronary artery disease, type 2 diabetes, QT-interval, body mass index/obesity, lipid traits, glycemic traits, and blood pressure; mitochondrial markers; HLA markers; sex chromosome markers; and ancestry informative markers<sup>2, 3</sup>. Illumina software GenomeStudio (v1.7.4) was used to determine the genotype calls for each variant for each sample, and manual re-clustering was performed on all mitochondrial and Y chromosome variants. Data were stored and accessed by the Vanderbilt Computational Genomics Core for quality control and downstream analyses using BC Platforms (Espoo, Finland).

### 2.3. Statistical methods

Standard quality control metrics were generated using PLINKv1.07<sup>4</sup> and PLATOv0.84<sup>5</sup>.  $F_{ST}$  calculations were based on the Weir and Cockerham algorithm<sup>6</sup> implemented in PLATO. Allele frequencies and  $F_{ST}$  were calculated for CEU, YRI, JPN and CHB combined (ASN), and MEX unrelated samples separately. Linkage disequilibrium ( $r^2$ ) was calculated using independent samples stratified by race/ethnicity using Haploviewv4.2<sup>7</sup>.

## 3. Results

We genotyped 360 DNA samples from the International HapMap collection including 90 CEU, 90 YRI, 90 ASN, and 90 MEX on the Illumina MetaboChip. From the 360 samples, 358 (99%) samples were successfully genotyped. And, out of the targeted 196,725 genetic variants on the MetaboChip, we obtained data for 185,788 genetic variants for an overall pre-quality control call rate of 94.44%. From this initial dataset, we then performed quality control as outlined by Buyske et al<sup>2</sup> (Table1).

To examine potential population differences for genetic variants targeted by the MetaboChip, we first determined minor allele frequencies for every variant by HapMap population. As shown in Figure 1, the majority of variants for this custom BeadChip are polymorphic. More than one half (58% for ASN) to up to three-quarters (75% for YRI) of the alleles assayed by the MetaboChip occurred at greater than 1% frequency. Conversely, one quarter (24% for

YRI) to more than one-third (38% for ASN) of the variants were monomorphic in this small sample set.

We also calculated a fixation index,  $F_{ST}$ , for all pair-wise population comparisons.  $F_{ST}$  is an estimate of population differentiation ranging from 0 (no measureable genetic differentiation) to 1.0 (very great genetic differentiation), and its distribution for MetaboChip-targeted variants in HapMap samples is given in Figure 2. The majority (76%) of  $F_{ST}$  values are less than 0.15 for all genetic variant pair-wise population comparisons. The most population differentiation was observed between YRI and ASN. Conversely, the least population differentiation was observed between CEU and MEX.

Of the most highly differentiated SNPs ( $F_{ST} > 0.15$ ), we examined the degree to which alleles altered the expression or function of genes using annotation resources from the Genome-Wide Annotation Repository (<http://gwar.mc.vanderbilt.edu>). We defined two categories of SNP annotation for this analysis: predicted changes to protein function via SIFT and PolyPhen2 algorithms<sup>8,9</sup>, and prior associations to expression levels of nearby genes<sup>10,11</sup>. The total number of SNP and gene annotations is shown in tables 2 and 3.

Using this collection of genes associated to differentiated SNPs through functional annotations, we performed gene enrichment analysis to identify specific biological mechanisms that likely have altered function between ethnic groups. This analysis revealed multiple pathways showing differences between CEU and MEX and CEU and ASN populations. KEGG pathways showing significant adjusted p-values ( $p < 0.05$ ) are shown in Table 4.

Notably, the most significantly enriched pathways between CEU and MEX indicate a dramatic difference in the functional properties of glutathione and drug metabolism through cytochrome P450. Enrichment of these three pathways is the result of a single SNP – rs1010167 -- altering expression of three genes, *GSTM1* ( $p=3.88e-7$ ), *GSTM2* ( $p=1.54e-7$ ), and *GSTM4* ( $p=8.44e-7$ )<sup>11</sup>. This SNP falls within a region of chromatin that has been functionally categorized as an active promoter by the analysis of Ernst et al. in multiple cell types<sup>12</sup>, and is confirmed to bind multiple proteins via ChIP-seq data as reported by the HaploREG database<sup>13</sup>. rs1010167 was not previously genotyped by the HapMap phase III project.

Remaining pathways showing high differentiation in the CEU/ASN and CEU/MEX comparisons are largely immune-related, and are driven mostly by functional changes to the Major Histocompatibility Complex (MHC) found on chromosome 6. Interestingly, there were no significant pathways found for differentiated functional SNPs involving YRI comparisons.

To illustrate the fine-mapping potential of densely targeted regions on the MetaboChip, we calculated linkage disequilibrium ( $r^2$ ) by HapMap population for the CELSR2/PSRC1/SORT1 locus known to be associated with low-density lipoprotein cholesterol levels from GWA studies in European-descent populations<sup>14-16</sup>. Consistent with the observations of Buyske et al<sup>17</sup> in samples from African American and Swedish participants, we observed less LD in YRI compared with CEU for this genomic region. To extend the observations made by Buyske et al, we examined LD for the same genomic region in HapMap samples of Asian and Mexican ancestry (Figure 3 c,d). As observed with minor allele frequency and  $F_{ST}$ , the CEU and MEX populations displayed similar levels of LD for this genomic region. In contrast, the ASN population had LD patterns that were distinct from CEU, YRI, and MEX LD patterns. For the ASN population, the CELSR2/PSRC1/SORT1 locus contained strong pair-wise LD statistics punctuated by weak LD.

## 4. Conclusions

We demonstrate here that the MetaboChip custom BeadChip produces high-quality data for diverse populations from the International HapMap Project. We further show that the majority of variants observed in all populations considered were common and that a sizeable fraction of variants were monomorphic. Finally, we demonstrate population differences in both allelic diversity and LD patterns, both of which will impact the effectiveness of fine-mapping efforts that employ this BeadChip in the post-GWAS era.

Many of the observations reported here were expected based on population genetics theory and recent empirical genome-wide data from the International HapMap Project<sup>18, 19</sup> and 1000 Genomes Project<sup>20</sup>. That is, as expected, the greatest population differentiation (as measured by  $F_{ST}$ ) was observed between African-descent and Asian-descent populations<sup>21</sup>. However, other observations such as the proportion of common and rare variants did not follow expectations given the bias in genetic variant selection for this custom BeadChip<sup>22</sup>. From our  $F_{ST}$  analysis, we also observe significant differentiation of functional alleles within drug metabolism and auto-immune associated pathways between CEU and ASN/MEX populations. These variants may explain some aspects of ethnic differences in HLA-based autoimmune disease susceptibility, and indicates that cytochrome P450 drug metabolism may be altered in individuals of Mexican ancestry.

A major limitation of this study is sample size. With only 60 to 90 independent samples per HapMap population, our ability to observe rare alleles targeted by the MetaboChip was limited for any HapMap population. Indeed, although the shape of the allelic distribution was similar, proportionally more variants in our dataset were classified as common or monomorphic compared with Buyske et al reflecting our limited ability to observe rare variants. Larger sample sizes will be required to take advantage of the full range of the allelic spectrum targeted by the MetaboChip for fine mapping.

A final observation made here that will impact fine-mapping efforts is the extent of LD for an LDL-C associated region across populations. As Buyske et al<sup>2</sup> noted, the breakdown of LD in African Americans for this region (and West Africans here) will be useful in identifying the true risk variant in a region with high LD in European populations. However, we note in ASN that the same genomic region has very high LD and thus this custom BeadChip may not fine map equally well for all targeted GWAS-identified regions for all populations. Because this custom BeadChip was designed using early iterations of the 1000 Genomes Project data, additional iterations of chips designed for fine mapping will be required to capture the latest genetic diversity data now emerging in non-European descent populations from later releases of the 1000 Genomes Project.

## Acknowledgments

This work was supported by NIH U01 HG004798 and its ARRA supplements. The Vanderbilt University Center for Human Genetics Research, Computational Genomics Core provided computational and/or analytical support for this work.

## References

1. Matisse TC, Ambite JL, Buyske S, Carlson CS, Cole SA, Crawford DC, Haiman CA, Heiss G, Kooperberg C, Marchand LL, Manolio TA, North KE, Peters U, Ritchie MD, Hindorf LA, Haines JL. The Next PAGE in Understanding Complex Traits: Design for the Analysis of Population Architecture Using Genetics and Epidemiology (PAGE) Study. *American Journal of Epidemiology*. 2011; 174(7):849–859. [PubMed: 21836165]



2. Buyske S, Wu Y, Carty CL, Cheng I, Assimes TL, Dumitrescu L, Hindorff LA, et al. Evaluation of the MetaboChip Genotyping Array in African Americans and Implications for Fine Mapping of GWAS-Identified Loci: The PAGE Study. *PLoS ONE*. 2012; 7(4):e35651. [PubMed: 22539988]
3. Center for Statistical Genetics. MetaboChip SNP details. University of Michigan; Jul 26. 2012 2012
4. Purcell S, Neale B, Todd-Brown K, Thomas L, Ferreira MA, Bender D, Maller J, Sklar P, de Bakker PI, Daly MJ, Sham PC. PLINK: a tool set for whole-genome association and population-based linkage analysis. *Am J Hum Genet*. 2007; 81(3):559–575. [PubMed: 17701901]
5. Grady BJ, Torstenson E, Dudek SM, Giles J, Sexton D, Ritchie MD. Finding unique filter sets in PLATO: a precursor to efficient interaction analysis in GWAS data. *Pac Symp Biocomput*. 2010:315–326. [PubMed: 19908384]
6. Weir BS, Cockerham CC. Estimating F-statistics for the analysis of population structure. *Evolution*. 1984; 38(1358):1370.
7. Barrett JC, Fry B, Maller J, Daly MJ. Haploview: analysis and visualization of LD and haplotype maps. *Bioinformatics*. 2005; 21(2):263–265. [PubMed: 15297300]
8. Ng PC, Henikoff S. Predicting deleterious amino acid substitutions. *Genome Res*. 2001; 11(5):863–874. [PubMed: 11337480]
9. Adzhubei IA, Schmidt S, Peshkin L, Ramensky VE, Gerasimova A, Bork P, Kondrashov AS, Sunyaev SR. A method and server for predicting damaging missense mutations. *Nat Methods*. 2010; 7(4):248–249. [PubMed: 20354512]
10. Veyrieras JB, Kudravalli S, Kim SY, Dermitzakis ET, Gilad Y, Stephens M, Pritchard JK. High-resolution mapping of expression-QTLs yields insight into human gene regulation. *PLoS Genet*. 2008; 4(10):e1000214. [PubMed: 18846210]
11. Stranger BE, Forrest MS, Dunning M, Ingle CE, Beazley C, Thorne N, Redon R, Bird CP, de GA, Lee C, Tyler-Smith C, Carter N, Scherer SW, Tavare S, Deloukas P, Hurler ME, Dermitzakis ET. Relative impact of nucleotide and copy number variation on gene expression phenotypes. *Science*. 2007; 315(5813):848–853. [PubMed: 17289997]
12. Ernst J, Kheradpour P, Mikkelson TS, Shores N, Ward LD, Epstein CB, Zhang X, Wang L, Issner R, Coyne M, Ku M, Durham T, Kellis M, Bernstein BE. Mapping and analysis of chromatin state dynamics in nine human cell types. *Nature*. 2011; 473(7345):437–49.
13. Ward LD, Kellis M. HaploReg: a resource for exploring chromatin states, conservation, and regulatory motif alterations within sets of genetically linked variants. *Nucleic Acids Res*. 2012; 40(Database issue):D930–D934. [PubMed: 22064851]
14. Willer CJ, Sanna S, Jackson AU, Scuteri A, Bonnycastle LL, Clarke R, Heath SC, et al. Newly identified loci that influence lipid concentrations and risk of coronary artery disease. *Nat Genet*. 2008; 40(2):161–169. [PubMed: 18193043]
15. Teslovich TM, Musunuru K, Smith AV, Edmondson AC, Stylianou IM, Koseki M, Pirruccello JP, et al. Biological, clinical and population relevance of 95 loci for blood lipids. *Nature*. 2010; 466(7307):707–713. [PubMed: 20686565]
16. Kathiresan S, Melander O, Guiducci C, Surti A, Burt NP, Rieder MJ, Cooper GM, et al. Six new loci associated with blood low-density lipoprotein cholesterol, high-density lipoprotein cholesterol or triglycerides in humans. *Nat Genet*. 2008; 40(2):189–197. [PubMed: 18193044]
17. Buyske S, Wu Y, Carty CL, Cheng I, Assimes TL, Dumitrescu L, Hindorff LA, et al. Evaluation of the MetaboChip Genotyping Array in African Americans and Implications for Fine Mapping of GWAS-Identified Loci: The PAGE Study. *PLoS ONE*. 2012; 7(4):e35651. [PubMed: 22539988]
18. The International HapMap Consortium. A haplotype map of the human genome. *Nature*. 2005; 437(7063):1299–1320. [PubMed: 16255080]
19. A second generation human haplotype map of over 3.1 million SNPs. *Nature*. 2007; 449(7164):851–861. [PubMed: 17943122]
20. A map of human genome variation from population-scale sequencing. *Nature*. 2010; 467(7319):1061–1073. [PubMed: 20981092]
21. Integrating common and rare genetic variation in diverse human populations. *Nature*. 2010; 467(7311):52–58. [PubMed: 20811451]
22. Keinan A, Clark AG. Recent Explosive Human Population Growth Has Resulted in an Excess of Rare Genetic Variants. *Science*. 2012; 336(6082):740–743. [PubMed: 22582263]

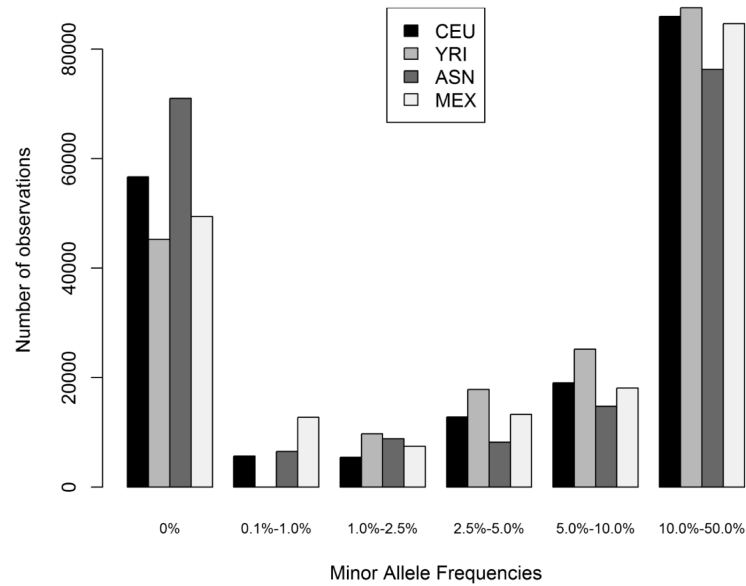


**Figure 1. Distribution of minor allele frequencies of genetic variants assayed by the MetaboChip, by HapMap population**

Allele frequencies were determined in the founder (unrelated) samples of Northern and Western European ancestry (CEU; n=60), West African ancestry (YRI; n=60), Asian ancestry (ASN; n=90), and Mexican ancestry (MEX; n=60). On the x-axis, genetic variant frequencies were binned as monomorphic, rare (0.1%-1%), less common (1-2.5%), and common (2.5-5%, 5-10%, and 10-50%) by population. Number of observations for each bin is given on the y-axis.

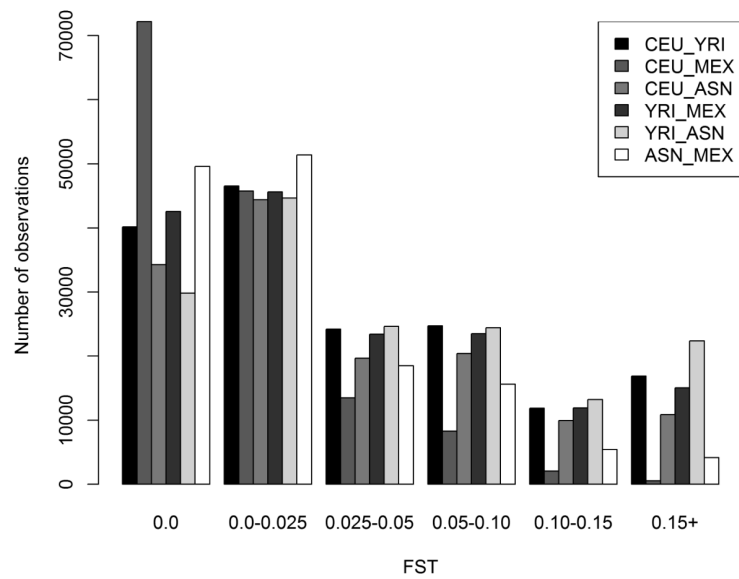


**Figure 2. Distribution of genetic differentiation ( $F_{ST}$ ) by HapMap population pairwise comparison**

$F_{ST}$ , a measure of population differentiation, was calculated per SNP in PLATO based on the Weir and Cockerham algorithm<sup>6</sup> for each HapMap population pair. Calculations were performed on unrelated samples of Northern and Western European ancestry (CEU;  $n=60$ ), West African ancestry (YRI;  $n=60$ ), Asian ancestry (ASN;  $n=88$ ), and Mexican ancestry (MEX;  $n=60$ ). On the x-axis,  $F_{ST}$  values were binned no difference (zero),  $>0.0-0.25$ ,  $>0.025-0.05$ ,  $>0.05-0.10$ ,  $>0.10-0.15$ ,  $>0.15$  by pair-wise population comparison. Number of observations for each bin is given on the y-axis.



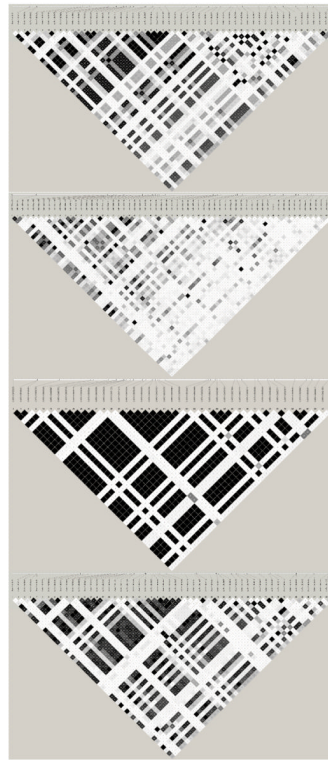


**Figure 3. Extent of linkage disequilibrium ( $r^2$ ) for 50kb region targeted by the MetaboChip containing genome-wide association study (GWAS)-identified *CELSR2/PSCR1/SORT1* by HapMap population**

Pair-wise linkage disequilibrium (LD) was calculated on unrelated samples using HaploView for European-descent [a]CEU; n=60], African [b]YRI; n=60], Asian [c]ASN; n=88], and Mexican [d]MEX; n=60] HapMap populations. For each LD plot, the genetic variants are labeled by chromosomal position at the top from 5' to 3'. Each square represents a pair-wise LD statistic and they are coded on a gray scale where black is perfect LD ( $r^2=1$ ) and white to gray is weak LD. The numbers in select squares represent the LD metric for that pair-wise comparison (for example, 1 is  $r^2=0.01$ ).

**Table 1**

Number of genetic variants removed from MetaboChip dataset after quality control, by criteria and HapMap population. We performed quality control steps appropriate for a single dataset as outlined by Buyske et al.<sup>2</sup>. Lower genotyping call rates were observed for YRI compared with other HapMap populations consistent with our observations for targeted genotyping in EAGLE (data not shown).

Criteria	SNP Failure Determination	# SNPs removed				
		CEU	YRI	CHB	JPN	MEX
Call Rate	< 0.95	14515	73445	11851	13585	14871
Mendelian Errors	> 1 (out of 30 trios)	97	10	0	0	144
Replication Errors	< 2	0	0	0	0	0
Hardy-Weinberg Equilibrium $p$ -value	< $1 \times 10^{-6}$	11	1	11	10	19
Discordant calls on EAGLE HapMap samples versus HapMap database	> 3 (out of 90 samples)	329	178	285	292	301

**Table 2**

Number of differentiated SNPs showing functional effects

Population Comparison	SIFT (Deleterious)	PolyPhen2 (Possibly or Probably Damaging)	Significant eQTL	Total functional SNPs*
ASN/MEX	6	12	202	218
YRI/ASN	23	50	786	844
YRI/MEX	15	33	620	654
CEU/ASN	10	24	445	474
CEU/YRI	13	28	598	631
CEU/MEX	0	1	15	16

\* this total accounts for overlap between annotations

**Table 3**

Number of distinct genes affected by differentiated SNPs

Population Comparison	SIFT (Deleterious)	PolyPhen2 (Possibly or Probably Damaging)	Significant eQTL	Total Genes Affected*
ASN/MEX	5	12	127	141
YRI/ASN	24	49	610	663
YRI/MEX	17	31	444	481
CEU/ASN	9	24	260	285
CEU/YRI	15	26	455	489
CEU/MEX	0	1	15	16

\* this total accounts for overlap between annotations

**Table 4**

Pathways with significant enrichment for highly differentiated functional alleles

Population Comparison	KEGG Pathway	Reference Genes	Observed Genes	Expected Genes	P-value	P-value (adjusted for multiple testing)
CEU/MEX	Glutathione metabolism	24	3	0.04	1.02E-05	9.47E-05
CEU/MEX	Metabolism of xenobiotics by Cytochrome P450	30	3	0.06	2.03E-05	9.47E-05
CEU/MEX	Drug metabolism - Cytochrome P450	29	3	0.05	1.83E-05	9.47E-05
CEU/ASN	Allograft rejection	26	6	0.83	0.0001	0.0007
CEU/ASN	Graft-versus-host disease	22	6	0.7	4.70E-05	0.0007
CEU/ASN	Systemic lupus erythematosus	54	9	1.71	4.35E-05	0.0007
CEU/ASN	Arginine and proline metabolism	17	5	0.54	0.0001	0.0007
CEU/ASN	Autoimmune thyroid disease	26	6	0.83	0.0001	0.0007
CEU/ASN	Antigen processing and presentation	29	6	0.92	0.0002	0.0013
CEU/MEX	Asthma	17	2	0.03	0.0004	0.0014
CEU/ASN	Type I diabetes mellitus	30	6	0.95	0.0003	0.0016
CEU/MEX	Intestinal immune network for IgA production	24	2	0.04	0.0009	0.0018
CEU/MEX	Type I diabetes mellitus	30	2	0.06	0.0013	0.0018
CEU/MEX	Allograft rejection	26	2	0.05	0.001	0.0018
CEU/MEX	Graft-versus-host disease	22	2	0.04	0.0007	0.0018
CEU/MEX	Autoimmune thyroid disease	26	2	0.05	0.001	0.0018
CEU/MEX	Antigen processing and presentation	29	2	0.05	0.0013	0.0018
CEU/ASN	Intestinal immune network for IgA production	24	5	0.76	0.0008	0.0039
CEU/ASN	Riboflavin metabolism	8	3	0.25	0.0016	0.007